

Crotamine is a novel cell-penetrating protein from the venom of rattlesnake *Crotalus durissus terrificus*

Alexandre Kerkis,^{*,§} Irina Kerkis,^{*,§} Gandhi Rádis-Baptista,[†] Eduardo B. Oliveira,[‡]
Angela M. Vianna-Morgante,^{*} Lygia V. Pereira,^{*} and Tetsuo Yamane[†]

^{*}Departamento de Biologia, Instituto de Biociências, Universidade de São Paulo, São Paulo, Brasil; [†]Laboratório de Toxinologia Molecular, Instituto Butantan, São Paulo, Brasil; [‡]Departamento de Bioquímica e Imunologia, Universidade de São Paulo, Ribeirão Preto, Brasil.

[§]These authors contributed equally to this work.

Corresponding author: Alexandre Kerkis, Departamento de Biologia, Instituto de Biociências, Universidade de São Paulo, Rua do Matão, 277, 05508-900, São Paulo, SP, Brasil. E-mail: akerkis@usp.br

ABSTRACT

Herein we report that crotamine, a small lysine- and cysteine-rich protein from the venom of the South American rattlesnake, can rapidly penetrate into different cell types and mouse blastocysts in vitro. In vivo, crotamine strongly labels cells from mouse bone marrow and spleen and from peritoneal liquid, as shown by fluorescent confocal laser-scanning microscopy. Nuclear localization of crotamine was observed in both fixed and unfixed cells. In the cytoplasm, crotamine specifically associates with centrosomes and thus allows us to follow the process of centriole duplication and separation. In the nucleus, it binds to the chromosomes at S/G2 phase, when centrioles start dividing. Moreover, crotamine appears as a marker of actively proliferating cells, as shown by 5-BrdU cell-proliferation assay. Crotamine in the micromolar range proved nontoxic to any of the cell cultures tested and did not affect the pluripotency of ES cells or the development of mouse embryos.

Key words: chromosomes • centrosomes • cell penetrating peptide

Peptides rich in basic arginine and lysine residues can be internalized by cells both in vitro (1–3) and in vivo (4–6) and thus have been used for the intracellular delivery of genes, therapeutic agents, and diagnostic probes (7–15). In addition, these peptides can be used as an efficient tool for genetic engineering of mammalian genomes (16) and provide an experimental model for studying mechanisms of translocation of macromolecules into cells, as well as those of cell aging and senescence (17, 18).

The number of known natural cell-penetrating peptides (CPPs) is limited, and they differ in primary sequence and penetrating capacity. The best-studied are Antp₄₃₋₅₈ from the Antennapedia homeodomain (1), Tat₄₈₋₆₀ from the transcription-activating factor of HIV (19, 20), and VP22 from the structural protein of Herpes simplex virus type I (HSV-1; 21). Antp₄₃₋₅₈ is internalized by cells in culture and is conveyed to the cell nucleus, but its use as a transduction molecule is limited because it transports only small peptides (18). VP22 localizes both in the cytoplasm and

nucleus of cell, where it interacts with microtubules, binds to chromatin, and then segregates to daughter cells (22). VP22 as well as HIV Tat₄₈₋₆₀ can transduce large proteins such as β -galactosidase into a wide variety of cell types (5, 7, 15, 23, 24). Moreover, HIV Tat₄₈₋₆₀ can translocate efficiently into quiescent cells (9). These properties make VP22 and HIV Tat₄₈₋₆₀ efficient delivery systems.

Crotamine is one of the main toxins in the venom of the South American rattlesnake (25) and is responsible for myonecrosis on snake envenomation (26). Crotamine shows high homology with other venom myotoxins (27, 28) and is similar to α - β -defensins and insect defensins (29, 30). It is a 42 amino acid-long cationic polypeptide (YKQCHKKGGHCFPKEKICLPPSSDFGKMDCRWRWKCCCKKGS—G), containing 11 basic residues (9 lysines, 2 arginines), and six cysteines, involved in 3 disulfide bonds. Crotamine size, primary sequence, and positive charge led us to investigate its cell- penetrating activity.

To access the penetrating capacity of crotamine, we used murine embryonic stem cells (ES), which are derived from the inner cell mass of blastocysts and are known to be pluripotent (31, 32). An important feature of ES cells is that they can be induced to undergo a differentiation program in vitro. When cultured in suspension, they spontaneously form aggregates of differentiating cells known as “embryoid bodies” (Ebs; 33). During their formation, the Ebs pass through different stages equivalent to early organogenesis. Between Days 3 and 9, Ebs contain precursors of hematopoietic, endothelial, muscular, and neuronal cell lineages (34–38). The developmentally regulated embryonic stage-specific genes are expressed during this period as in a normal embryo (39). Thus, ES cells represent an adequate model to investigate the penetrating capacity of peptides in pluripotent and differentiating cells.

We evaluated cytotoxicity of crotamine in murine ES cells. In addition, embryotoxicity was tested in vitro, in the pre-implantation stages (morulae-blastocysts) of mouse embryo. The uptake of Cy3-conjugated crotamine (Cy3-crotamine) and its intracellular localization were analyzed in different human cells and murine undifferentiated and differentiating ES cells, as well as, in vivo, in mouse cells from bone marrow, spleen and the peritoneal cavity.

MATERIALS AND METHODS

Purification of crotamine

Crotalus durissus terrificus venom was extracted from snakes maintained at the FMRP serpentarium, São Paulo University, and dried under vacuum. Crude venom (600 mg) were dissolved in 5 ml of 0.25 M ammonium formate buffer, pH 3.5, and the bulk of crotoxin, the major venom component, was eliminated by slow-speed centrifugation as a heavy precipitate that formed upon slow addition of 20 ml of cold water to the solution. Tris-base 1 M was then added drop-wise to the supernatant to raise the pH to 8.8, and the solution was applied to a CM-Sepharose FF (1.5×4.5 cm; Amersham-Biosciences, Buckinghamshire, UK) column equilibrated with 0.04 M Tris-C1 buffer, pH 8.8, containing 0.064 M NaCl. After the column was washed with 100 ml of equilibrating solution, crotamine was recovered as a narrow protein peak by raising the NaCl concentration of the diluting solution to 0.64 M. The material was thoroughly dialyzed against water (benzoylated membrane, cut off MW = 3000) and lyophilized. Amino acid analysis after acid hydrolysis of a sample (4 N MeSO₃H⁺0.1% tryptamine; 24 h at 115C^o) of a sample indicated yield of 72 mg (14.7 μ M) of crotamine (40) and trace amounts of Thr, Ala, and Val (purity >98%).

Labeling of crotamine with the fluorescent dye Cy3

Crotamine (1 mg) was covalently conjugated to the fluorescent dye Cy3 by using the Fluorolink Cy3 reactive dye (Amersham Biosciences). To verify whether crotamine was biologically active after labeling, mice were intraperitoneally injected with sublethal doses of 50 μ g of Cy3-crotamine (corresponding to 2.5 mg of toxin/kg body mass). The typical hind-limb paralysis was observed in less than 15 min after injection.

Cell culture

Mouse ES-cell line USP 1 (41), in passages 8–10, were grown onto a feeder layer of γ -irradiated mouse primary embryonic fibroblasts, in Dulbecco's modified Eagle's medium (DMEM; Invitrogen, Carlsbad, CA) supplemented with 15% of fetal calf serum (FCS; Invitrogen), 1 mM sodium pyruvate, 1% nonessential amino acid, 0.1 mM β -mercaptoethanol, and 1×10^3 U/ml murine leukemia inhibitory factor (ESGRO-LIF; Invitrogen). Human primary skin fibroblasts and a lymphoblastic cell line were cultured in DMEM and in RPMI, respectively, supplemented with 10% FCS without antibiotics. All cell cultures were maintained at 37°C in a humidified atmosphere with 5% CO₂. Human cell donors volunteered for this research, and informed consent was obtained according to the Institutional Ethics Committee requirements.

In vitro differentiation of ES cells

The “hanging drop” method (42), with some modification, was used to induce the differentiation of USP-1 cell line. Briefly, fibroblast feeder-free single-cell suspensions were obtained by harvesting the cells with 0.25% trypsin/EDTA (Invitrogen) from culture dishes, and 25 μ l drops (3.5×10^4 cells/ml) were placed onto the lids of 10 cm bacterial-grade culture dishes. The dishes were filled with 5 ml of phosphate-buffered saline and covered with the lids. After three days of “hanging drop” culture in the appropriate ES culture media without LIF, the cells formed aggregates—the Ebs—that were cultured for another two days in 35 mm plates coated with 1% agarose, at 37°C and 5% CO₂. On Day 5, Ebs were allowed to differentiate in a monolayer on microscope slides.

Embryotoxicity assay

The Ebs were obtained by the aforementioned “hanging drop” method by using medium containing crotamine at different concentrations (100 to 0.1 μ M), which was changed every 2–3 days. For the analysis of the toxin localization in developing Ebs, crotamine was replaced by Cy3-crotamine during the last 24 h of incubation. Murine compact morulae (8–16 cells) were flushed from oviducts and cultured for 24 h at 37°C with 5% CO₂ in individual microwells of a standard 96-microwell V-bottom plate (Corning, NY), in M16 medium (Sigma, St. Louis, MO) and Cy3-crotamine (1–0.1 μ M). After 24 h of cultivation, the number of normally developed blastocysts in control and experimental groups was counted.

Crotamine uptake

Semi-confluent cultures of pluripotent and differentiating ES cells, human diploid fibroblasts, and endothelial murine s-vec cells were grown onto microscope slides in 24-well plates in appropriate culture media. The cells were incubated 2–3 min to 72 h in the presence of Cy3-

crotamine at concentrations between 10 and 0.01 μM or in the presence of Cy3 dye diluted in 1 ml of PBS. In vivo, 1 ml of 1 μM Cy3-crotamine or control Cy3 dye in PBS was injected into mice (strain CD-1) intraperitoneally. After 3 h, the cells from bone marrow, spleen, and peritoneal liquid were isolated. Cells from peritoneal liquid were allowed to adhere for 1 h onto the microscope slides, in RPMI supplemented with 10% FCS without antibiotics at 37°C in a humidified atmosphere with 5% CO_2 . In all experiments cells were washed twice with ice-cold 0.1 M PBS (pH 7.4), fixed with 3.7% formaldehyde in PBS for 15 min, and washed twice in PBS. Microscope slides were mounted in PBS/glycerol (1:1) solution. Alternatively, unfixed cells were washed twice in PBS and immediately observed under confocal microscope.

Chromosome studies

Cy3-crotamine (1 μM) was added to the cultures of USP-1 ES cells, human primary fibroblasts, and lymphoblastic cells for 1, 3, 6, and 24 h. The cells were harvested and treated according to routine cytogenetic protocols without the addition of colchicine. Analysis was performed with a Zeiss II epifluorescence microscope. Digital images were acquired by using a cooled CCD camera (PCO, VC44) and were processed by means of ISIS software (MetaSystem)

Peptide competition assay

To evaluate Cy3-crotamine specific binding to chromatin and centrioles, 1 μM non-labeled crotamine was added to ES cells and murine embryonic fibroblasts for 15 min followed by addition of 1 μM Cy3-crotamine for another 15 min. A similar experiment was performed in vivo by injecting both labeled and unlabeled crotamine into mice. Cy3-crotamine (1 μM) for 15 min was used in controls. All animal procedures were performed in accordance with the institutional guidelines.

5-BrdU labeling and antibodies

The Cell Proliferation Kit (Amersham Biociences) was used to analyze internalization of Cy3-crotamine by actively proliferating cells in differentiating ES cell culture. Briefly, Ebs were obtained by the aforementioned “hanging drop” method at 10^6 cells/ml. Differentiating Ebs were treated with Cy3-crotamine (1 μM) and 5-bromo-2'-deoxyuridine (5-BrdU) at the final concentration of 10 $\mu\text{g}/\text{ml}$ for 2 h. After a 2 h post-labeling period, the Ebs were washed twice with ice-cold 0.1 M PBS (pH 7.4), fixed with 3.7% formaldehyde for 10 min, washed in PBS, and permeabilized in 0.1% triton X-100. Slides were incubated with primary FITC-conjugated anti-BrdU antibody 1:500 for 1 h, after blocking with 5% BSA.

Centrioles and spindle microtubules were fixed by following the above described protocol and were immunostained with monoclonal mouse FITC-conjugated anti- α -tubulin antibody 1:50 for 1 h (Sigma).

Confocal microscopy

An argon ion laser set at 488 nm for fluorescein isothiocyanate excitation was used, and the emitted light was filtered with a 515-nm-long pass filter in a laser-scan microscope (LSM 410, Zeiss). Sections were taken approximately at the mid-height level of cells. Photo multiplier gain and laser power were kept constant throughout each experiment.

RESULTS

Non-toxic concentrations of crotamine

Because pluripotency is a conspicuous feature of ES cells that can be lost in altered culture conditions, the effect of 10 and 0.1 μM of crotamine on the pluripotency of the mouse ES cell line USP-1 was tested during three passages. Alkaline phosphatase is active in the undifferentiated cells (43), and its activity was not altered when ES cells were maintained under crotamine treatment (data not shown). The dynamics of embryoid body (Ebs) formation were not impaired, as shown by the number of developed Ebs in experimental and control conditions ([Table 1](#)), as well as by the typical rhythmic contractions of the heart muscle observed on developmental day 8 (33, 44).

The susceptibility of murine ES and embryonic fibroblasts to crotamine concentrations between 1000 and 0.01 μM was assayed by clonogenicity (45). At concentrations of 10 μM and lower, crotamine exhibited no toxic effects, even after 72 h of exposure, and crotamine-treated cells successfully proliferated for more than 10 passages.

Embryotoxicity of crotamine was investigated by incubating 2.5-day post-coitum (d.p.c.) compact mouse morulae in the presence of 1 μM crotamine for 24 h and its uptake into developing blastocysts was evidenced by confocal microscopy ([Fig. 1A–C](#)). The number of compact morulae that developed into blastocysts was similar in both control and test groups ([Table 2](#)).

Cy3-crotamine uptake in vitro and in vivo

Cellular uptake of Cy3-crotamine at the non-toxic concentration of 1 μM was monitored by confocal microscopy after 5 min and 1, 3, 24, and 48 h treatment.

In vitro crotamine uptake was observed in human primary fibroblasts, lymphoblastic cells, murine embryonic stem (pluripotent and differentiated), and endothelial s-vec cells. Human fibroblasts were intensively labeled after 1 h of incubation with crotamine ([Fig. 2A](#)); supposedly dividing cells showed stronger signals ([Fig. 2B, C](#)). The pluripotent murine ES cells showed strong fluorescence within the islands composed by rounded up, juxtaposed cells growing onto a feeder layer of inactivated mouse fibroblasts; some of the islands were weakly labeled ([Fig. 2D, E](#)). A weak background of fluorescent signals was seen in control ES cultures stained by Cy3 dye ([Fig. 2F](#)).

In vivo uptake of crotamine was studied by intraperitoneal injection of Cy3-crotamine into CD-1 mice. After 3 h, cells isolated from bone marrow, spleen, and peritoneal liquid were allowed to adhere onto slides for 30 min and were fixed. Strong fluorescence was observed in peritoneal liquid cells ([Fig. 2G–I](#)) and in bone marrow cells ([Fig. 3E–G](#)). In control Cy3-injected mice, only weak background fluorescence was observed (data not shown).

The cells internalize crotamine within the first 5 min after its addition. The number of labeled cells did not seem to increase with longer exposure times to crotamine, which reached a maximum after about 3 h of treatment. Cell labeling was no longer detected 16–24 h after removal of fluorescent crotamine from the culture medium. Parallel experiments demonstrated

that Cy3-conjugated crotamine was efficiently internalized at concentrations as low as 10 nM at 37 but not at 4°C.

Crotamine nuclear localization

Cy3-crotamine was visualized in the nuclear and perinuclear regions in different types of bone marrow cells ([Fig. 3A–G](#)). DNA DAPI-staining partially overlapped the crotamine localization in the nuclei ([Fig. 3C, D](#)).

When injection of non-labeled crotamine was followed by an injection of Cy3-crotamine, after another 15 min, the fluorescence could be seen restricted to the cytoplasm, preferentially to the perinuclear space, which indicated a saturation of binding sites by non-labeled crotamine within the nucleus ([Fig. 3H](#)). The same results were observed in human fibroblast by treating the cells with non-labeled and Cy3-crotamine (data not shown).

During mitosis, Cy3-crotamine was visualized on the metaphase chromosomes in human lymphoblastic cells stained with DAPI ([Fig. 3I–K](#)). Interestingly, a differential longitudinal chromosome pattern was evidenced ([Fig. 3I](#), inset).

Nuclear localization of Cy3-crotamine was studied in unfixed cells. Three hours after crotamine injection into mice, cells from peritoneal liquid showed fluorescence in the cytoplasm and nuclei ([Fig. 4A–C](#)). A partial overlap of DNA DAPI-staining and crotamine labeling was observed in the nuclei of unfixed bone marrow cells on slides mounted with DAPI/antifade solution and immediately analyzed under fluorescence microscopy ([Fig. 4D–F](#)).

Crotamine as a marker of centrioles and during the cell cycle

The Cy3-crotamine also seems to function as a marker of the centrosome cycle. [Fig. 5A](#) shows centrioles from peritoneal liquid cells labeled with Cy3-crotamine at different phases of cell cycle. To analyze the association of crotamine with centrioles in ES cells, we used anti- α -tubulin antibody to highlight out the spindle and the esters, small star-like structures formed by new microtubules growing out from centrosomes during mitosis ([Fig. 5B](#)). Cy3-crotamine co-localizes with esters immunostained by anti-tubulin, indicating its centrosomes association ([Fig. 5C](#)). In addition, Cy3-crotamine labels the chromosomes attached to the α -tubulin immunostained spindles ([Fig. 5C](#)).

The processes of centrosome duplication and separation were observed in Cy3-crotamine-treated peritoneal liquid cells ([Fig. 5D–S](#)). Initially, the centrioles pair and associated centrosome matrix were observed as a single complex ([Fig. 5D–F](#)). In S/G₂, the two centrioles could be seen as they started to move apart ([Fig. 5G–L](#)). At metaphase ([Fig. 5M–O](#)) and anaphase ([Fig. 5P–S](#)), the centrioles were observed in the opposite poles. In S/G₂ phase the fluorescent signal appeared on the chromosomes ([Fig. 5G–I](#)) and became very strong at metaphase ([Fig. 5M–O](#)).

Crotamine as a marker of actively proliferating cells

The intensity of Cy3-crotamine cell labeling varied ([Figs. 1A–E](#) and [3E–G](#)). This finding was striking when ES cells were induced to differentiate through Ebs: A six-day monolayer culture of a differentiating Eb was treated with Cy3-crotamine for 24 h and undifferentiated ES cells within the Eb, which supposedly were actively proliferating, appeared strongly labeled ([Fig. 6A](#)).

A 5-BrdU-proliferation assay was used to investigate whether crotonamine preferentially labels actively proliferating cells in differentiating Ebs. Cy3-crotonamine was added together with 5-BrdU into cultures of differentiating Ebs. 5-BrdU incorporation into DNA during replication was monitored by anti-BrdU antibody immunostaining. Although an intensive crotonamine labeling was observed in the areas of actively proliferating ES cells as evidenced by 5-BrdU incorporation, a weak Cy3-fluorescence was seen in the areas of predominantly non-dividing cells (Fig. 6B–D). Crotonamine and 5-BrdU had a nuclear localization in the actively proliferating cells (Fig. 6E–G), although overlapping was not complete (Fig. 6H), indicating different sites of interaction of crotonamine and 5-BrdU.

DISCUSSION

ES cells were used to study the toxicity of crotonamine, a toxin from the rattlesnake venom. Crotonamine in micromolar concentrations did not have any toxic effect on ES cells *in vitro*. We also demonstrated that it did not inhibit Ebs formation or ES cell differentiation into contracting myocardium and that it was non-toxic for developing mouse blastocysts.

We investigated crotonamine internalization *in vitro* in different cell lines (human primary fibroblasts, lymphoblastic cells, murine embryonic stem, and endothelial s-vec cells), as well as *in vivo* in various cell types isolated from mouse. Internalization was always effective, and cells showed strong labeling within 5 min of treatment with Cy3-crotonamine, a feature shared with other cell-penetrating proteins (46). Signals of similar intensities were observed in cells incubated with 1 μ M Cy3-crotonamine for 1–48 h. Cells incubated with Cy3-crotonamine at concentrations as low as 10 nM were also rapidly and intensively labeled (data not shown).

Once internalized, Cy3-crotonamine was observed in the perinuclear space and in the cell nucleus. Its nuclear localization was confirmed by DAPI staining and by a peptide competition assay demonstrating that Cy3-crotonamine was not translocated into the nucleus when crotonamine sites were previously saturated with non-labeled crotonamine. Because fixation is known to produce artificial nuclear localization of cationic peptides (47), crotonamine penetration into the nuclei was studied in unfixed and fixed cells, and it was observed in both cases.

It is known that the nuclear translocation process resides on lysine- and arginine-rich nuclear localization signals (NLSs; 16, 17, 48–50). The most frequent motif is one or two short segments enriched in positively charged amino acids, the precise sequence varying in different NLSs (51), and whose presence is necessary but not sufficient for a peptide to display a nuclear localization activity (3). Because no sequence conservation among NLSs is apparent, shape and charge density seem to be determinants of the nuclear localization activity. Crotonamine's three disulfide bridges may confer to this molecule a structural configuration and charge distribution that result in unique penetrating properties. Crotonamine has two putative NLS motifs, Cro₂₋₁₈ (KQCHKKGGHCFPKEKIC) and Cro₂₇₋₃₉ (KMDCRWRWKCCCKK), which could be responsible for its nuclear penetration activity or, alternatively, they both could constitute a bipartite signal, as in the case of nucleoplasmin (51).

Crotonamine was shown to bind to DAPI-stained and 5-BrdU-labeled metaphase chromosomes. It seems to bind to chromosomes in the S/G2 phase, and in G2/M phase, during chromosome condensation when the fluorescent labeling becomes evident on all chromosomes. At the end of telophase, crotonamine is restricted to the cytoplasm. After 16–24 h of its removal from cell culture

medium, crotamine is not detected in cells. In this regard, crotamine differs from herpes simplex VP22 protein, which also binds to chromatin after internalization and segregates to daughter cells (22).

Crotamine was also demonstrated to specifically associate with centrosomes by simultaneous anti-tubulin immunostaining and crotamine labeling of esters, thus allowing the position of the cell in the cell cycle to be assigned. As a centriolar marker, it appears as a tool to monitor unfixed human tumor cells characterized by abnormally high number of centrosomes (52). Compared with penetrating peptides so far reported (1, 19–21), only crotamine was shown to selectively label actively proliferating living cells, both in vivo and in vitro.

The mechanism of uptake of cationic cell-penetrating peptides is still unclear and has recently been critically re-evaluated concerning the involvement of endocytosis in the process (47, 53). The inability of crotamine to penetrate into cells at a low temperature is indicative that the internalization of this protein involves endocytosis. Different toxins from bacteria and plants penetrate into cells using cellular mechanism or carrying their own translocation apparatus, but in both cases endocytosis is a requirement for penetration (54). However, crotamine appears to have a complex penetration mechanism as evidenced by selective labeling pattern, which deserves further investigation.

Crotamine was characterized as a cell-penetrating protein with nuclear localization in vitro and in vivo. The nature of crotamine interaction with chromatin is unclear, but our morphological data indicate that the mechanisms involved differ from those of DAPI or 5-BrdU. It differs from other CPPs, thus crotamine was qualified as a marker of cell cycle based on the process of centrioles duplication and separation. Moreover, crotamine was shown to be a marker for actively proliferating cells.

ACKNOWLEDGMENTS

We thank C. J. Laure and L. H. A. Pedrosa for the generous supply of *C. d. terrificus* venom; Marco Mello for providing embryos and adult mice; and Waldir Caldeira for technical assistance with fluorescent confocal microscopy. FAPESP and CNPq supported this work.

REFERENCES

1. Derossi, D., Joliot, A. H., Chassaing, G., and Prochiantz, A. (1994) The third helix of the Antennapedia homeodomain translocates through biological membranes. *J. Biol. Chem.* **269**, 10444–10450
2. Fawell, S., Seery, J., Daikh, Y., Moore, C., Chen, L. L., Pepinsky, B., and Barsoum, J. (1994) TAT-mediated delivery of heterologous proteins into cells. *Proc. Natl. Acad. Sci. USA* **91**, 664–668
3. Vivés, E., Brodin, P., and Lebleu, B. (1997) A truncated HIV-1 Tat protein basic domain rapidly translocates through the plasma membrane and accumulates in the cell nucleus. *J. Biol. Chem.* **272**, 16010–16017
4. Derossi, D., Chassaing, G., and Prochiantz, A. (1998) Trojan peptides: the penetratin system for intercellular delivery. *Trends Cell Biol.* **8**, 84–87

5. Schwarze, S. R., Ho, A., Vocero-Akbani, A., and Dowdy, S. F. (1999) *In vivo* protein transduction: delivery of a biologically active protein into the mouse. *Science* **285**, 1569–1572
6. Caron, N. J., Torrente, Y., Camirand, G., Bujold, M., Chapdelaine, P., Leriche, K., Bresolin, N., and Tremblay, J. P. (2001) Intercellular delivery of a TAT-eGFP fusion protein into muscle cells. *Mol. Ther.* **3**, 310–318
7. Dilber, M., Phelan, A., Aints, A., Mohamed, A., Elliott, G., Edvard Smith, C., O'Hare, P. (1999). Intercellular delivery of thymidine kinase prodrug activating enzyme by the Herpes simplex's virus protein, VP22. *Gene Ther.* **6**, 12–21
8. Hawiger, J. (1999) Noninvasive intracellular delivery of functional peptides and proteins. *Curr. Opin. Chem. Biol.* **3**, 89–94
9. Schwarze, S. R., Hruska, K. A., and Dowdy, S. F. (2000) Protein transduction: unrestricted delivery into the cells? *Trends Cell Biol.* **10**, 290–296
10. Morris, M. C., Chaloin, L., Heitz, F., and Divita, G. (2000) Translocating peptides and proteins and their use for gene delivery. *Curr. Opin. Biotechnol.* **11**, 461–466
11. Futaki, S., Suzuki, T., Ohashi, W., Yagami, T., Tanaka, S., Ueda, K., and Sugiura, Y. (2001) Arginine-rich peptides. An abundant source of membrane-permeable peptides having potential as carriers for intracellular protein delivery. *J. Biol. Chem.* **276**, 5836–5840
12. Embury, J., Klein, D., Pileggi, A., Ribeiro, M., Jayaraman, S., Molano, R. D., Fraker, C., Kenyon, N., Ricordi, C., Inverardi, L., et al. (2001) Proteins linked to a protein transduction domain efficiently transduce pancreatic islets. *Diabetes* **50**, 1706–1713
13. Yoon, H.-Y., Lee, S. H., Cho, S. W., Lee, J. E., Yoon, C. S., Park, J., Kim, T. U., and Choi, S. Y. (2002) TAT-mediated delivery of human glutamate dehydrogenase into PC12 cells. *Neurochem. Int.* **41**, 37–42
14. Yuan, J., Kramer, A., Eckerdt, F., Kaufmann, M., and Sterbhardt, K. (2002) Efficient internalization of the Polo-box of Polo-like kinase 1 fused to an Antennapedia peptide results in inhibition of cancer cell proliferation. *Cancer Res.* **62**, 4186–4190
15. Cashman, S. M., Sadowski, S. L., Morris, D. J., Frederick, J., and Kumar-Singh, R. (2002) Intercellular trafficking of adenovirus-delivered HSV VP22 from the retinal pigment epithelium to the photoreceptor - Implication for gene therapy. *Mol. Ther.* **6**, 813–823
16. Peitz, M., Pfannkuche, K., Rajewsky, K., and Edenhofer, F. (2002) Ability of the hydrophobic FGF and basic TAT peptides to promote cellular uptake of recombinant Cre recombinase: A tool for efficient genetic engineering of Mamm Genomes. *Proc. Natl. Acad. Sci. USA* **99**, 4489–4494
17. Futaki, S. (2002) Arginine-rich peptides: potential for intracellular delivery of macromolecules and the mystery of the translocation mechanisms. *Int. J. Pharm.* **245**, 1–7

18. Ford, K. G., Darling, D., Souberbielle, B., and Farzaneh, F. (2000) Protein transduction: a new tool for the study of cellular ageing and senescence. *Mech. Ageing Dev.* **121**, 113–121
19. Green, M., and Loewenstein, P. M. (1988) Autonomous functional domain of chemically synthesized human immunodeficiency virus tat *trans*-activator protein. *Cell* **55**, 1179–1188
20. Frankel, A., and Pabo, C. (1988) Cellular uptake of the tat protein from human immunodeficiency virus. *Cell* **55**, 1189–1193
21. Elliott, G., and O'Hare, P. (1997). Intercellular trafficking and protein delivery by a herpes virus structural protein. *Cell* **88**, 223–233
22. Martin, A., O'Hare, P., McLauchlan, J. and Elliott, G. (2002). Herpes simplex's virus tegument protein VP22 contains overlapping domains for cytoplasmic localization, microtubule interaction, and chromatin binding. *J. Virol.* **76**, 4961–4970
23. Nagahara, H., Vocero-Akbani, A., Snyder, E., Ho, A., Latham, D., Lissy, N., BeckerHapak, M., Ezhevsky, S., Dowdy, S. (1998). Transduction of full length TAT fusion proteins into mammalian cells: TAT-p27^{kip1} induces cell migration. *Nat. Med.* **4**, 1449–1452
24. Phelan, A., Elliott, G., and O'Hare, P. (1998) Intercellular delivery of functional p53 by the herpes virus protein VP22. *Nat. Biotechnol.* **16**, 440–443
25. Rádis-Baptista, G., Oguiura, N., Hayashi, M. A. F., Camargo, M. E., Grego, K. F., Oliveira, E. B., and Yamane, T. (1999) Nucleotide sequence of crotamine isoform precursors from a single South American rattlesnake (*Crotalus durissus terrificus*). *Toxicon* **37**, 973–984
26. Bieber, A. L., and Nedelkov, D. (1997) Structural, biological and biochemical studies of myotoxin a and homologous myotoxins. *J. Toxicol.-. Toxin Rev.* **16**, 33–52
27. Ownby, C. L., Cameron, M. S., and Tu, A. T. (1976) Isolation of myotoxin component from rattlesnake (*Crotalus viridis viridis*) venom. *Am. J. Pathol.* **85**, 149–166
28. Fox, J. W., Elzinga, M., and Tu, A. T. (1979) Amino acid sequence and disulfide bond assignment of myotoxin-a isolated from the venom of prairie rattlesnake (*Crotalus viridis viridis*). *Biochemistry* **18**, 678–684
29. Ganz, T., and Lehrer, R. I. (1998) Antimicrobial peptides of vertebrates. *Curr. Opin. Immun* **10**, 41–44
30. Dimarcq, J. L., Bulet, P., Hetru, C., and Hoffmann, J. (1998) Cysteine-rich antimicrobial peptides in vertebrates. *Biopolymers* **47**, 465–477
31. Evans, M., and Kaufman, M. (1981) Establishment in culture of pluripotential cells from mouse embryos. *Nature* **292**, 154–156
32. Martin, G. R. (1981) Isolation of a pluripotent cell line from early mouse embryos cultured in medium conditioned by teratocarcinoma stem cells. *Proc. Natl. Acad. Sci. USA* **78**, 634–638

33. Doetschman, T., Eistetter, H., Katz, M., Schmidt, W., and Kemler, R. (1985) The *in vitro* development of blastocyst-derived embryonic stem cell lines: formation of visceral yolk sac, blood islands and myocardium. *J. Emb. Exp. Morph.* **87**, 27–45
34. Maltsev, V. A., Wobus, A. M., Rohwedel, J., Bader, M., and Hescheler, J. (1994) Cardiomyocytes differentiated *in vitro* from embryonic stem cells developmentally express cardiac-specific genes and ionic currents. *Circ. Res.* **75**, 233–244
35. Keller, G. M. (1995) In vitro differentiation of embryonic stem cells. *Curr. Opin. Cell Biol.* **7**, 862–869
36. Bain, G., Kitchens, D., Yao, M., Huettner, J. E., and Gottlieb, D. I. (1995) Embryonic stem cells express neuronal properties in vitro. *Dev. Biol.* **168**, 342–357
37. Fraichard, A., Chassande, O., Bilbaut, G., Dehay, C., Savatier, P., and Samarut, J. (1995) *In vitro* differentiation of embryonic stem cells into glial cells and functional neurons. *J. Cell Sci.* **108**, 3181–3188
38. Bautch, V. L., Stanford, W. L., Rapoport, R., Russel, S., Byrum, R. S., and Futch, T. A. (1996) Blood island formation in attached cultures of murine embryonic stem cells. *Dev. Dyn.* **205**, 1–12
39. Leahy, A., Xiong, J. W., Kuhnert, F., and Stuhlmann, H. (1999) Use of developmental marker genes to define temporal and spatial patterns of differentiation during embryoid body formation. *J. Exp. Zool.* **284**, 67–81
40. Laure, C. J. (1975) Die primärstruktur des crotamins. *Hoppe Seylers Z. Physiol. Chem.* **356**, 213–215
41. Soukoyan, M. A., Kerkis, A. Y., Mello, M. R. B., Kerkis, I. E., Visintin, J. A., and Pereira, L. V. (2002) Establishment of new murine embryonic stem cell lines for the generation of mouse models of human genetic diseases. *Braz. J. Med. Biol. Res.* **35**, 535–542
42. Wobus, A. M., Wallukat, G., and Hescheler, J. (1991) Pluripotent mouse embryonic cells are able to differentiate into cardiomyocytes expressing chronotropic responses to adrenergic and cholinergic agents and Ca²⁺ channel blockers. *Differentiation* **48**, 173–182
43. Talbot, N. C., Rexrod, C. E., Pursel, V., and Powell, A. M. (1993) Alkaline phosphatase staining of pig and sheep epiblast cells in culture. *Mol. Reprod. Dev.* **36**, 139–147
44. Scholz, G., Pohl, I., Genschow, E., Klemm, M., and Spielmann, H. (1999) Embryotoxicity screening using embryonic stem cells *in vitro*: correlation to *in vivo* teratogenicity. *Cell. Tiss. Org.* **165**, 203–211
45. Wilson, A. P. Cytotoxicity and viability assays. (1986). In *Animal Cell Culture. A Practical Approach*, Freshney, R. I ed. IRL Press, Oxford; pp. 182–216
46. Lindgren, M., Hällbrink, M., Prochiantz, A., and Langel, Ü. (2000) Cell-penetrating peptides. *Trends Pharmacol. Sci.* **21**, 99–103

47. Richard, J. P., Melikov, K., Vives, E., Ramos, C., Verbeure, B., Gait, M. J., Chernomordik, L. V., and Lebleu, B. (2003) Cell-penetrating peptides. A re-evaluation of the mechanisms of cellular uptake. *J. Biol. Chem.* **278**, 585–590
48. Kalderon, D., Roberts, B. L., Richardson, W. D., and Smith, A. E. (1984) A short amino acid sequence able to specify nuclear location. *Cell* **39**, 499–509
49. Kaffman, A., and O’Shea, E. K. (1999) Regulation of nuclear localization: a key to a door. *Annu. Rev. Cell Dev. Biol.* **15**, 291–339
50. Wenthe, S. R. (2000) Gatekeepers of the nucleus. *Science* **288**, 1374–1377
51. Robbins, J., Dilworth, S. M., Laskey, R. A., and Dingwall, C. (1991) Two interdependent basic domains in nucleoplasmin nuclear targeting sequence: identification of a class of bipartite nuclear targeting sequences. *Cell* **64**, 615–623
52. Fisk, H. A., Mattison, C. P., and Winey, M. (2002) Centrosomes and tumor suppressors. *Mol. Cell. and Dev. Biol* **14**, 700–705
53. Drin, G., Cottin, S., Blanc, E., Rees, A. R., and Temsamani J. (2003). Studies on the internalisation mechanism of cationic cell-penetrating peptides. *J. Biol. Chem.* (Epub ahead of print)
54. Olsnes, S., Klingenberg, O. and Wiedlocha A. Transport of exogenous growth factors and cytokines to the cytosol and to the nucleus. (2003). *Physiol. Rev.* **83**, 163–182

Received January 16, 2004; accepted May 25, 2004.

Table 1

Number of embryonic stem (ES) cell aggregates that developed into embryoid bodies (Ebs) after prolonged crotamine treatment.

<i>Type of Ebs</i>	<i>Crotamine concentrations</i>		
	10 μ M	0.1 μ M	Control
3-Day ES cell aggregates	12	17	14
11-Day Ebs	8 (67%)	12 (70%)	10 (71%)

Table 2**Number of morulae that developed into blastocysts after exposure to 1 μ M crotamine for 24 h.**

	<i>Morulae (8–16 cells)</i>	<i>Blastocysts</i>
Crotamine-treated	80	64 (80%)
Control	86	60 (69.7 %)

Fig. 1

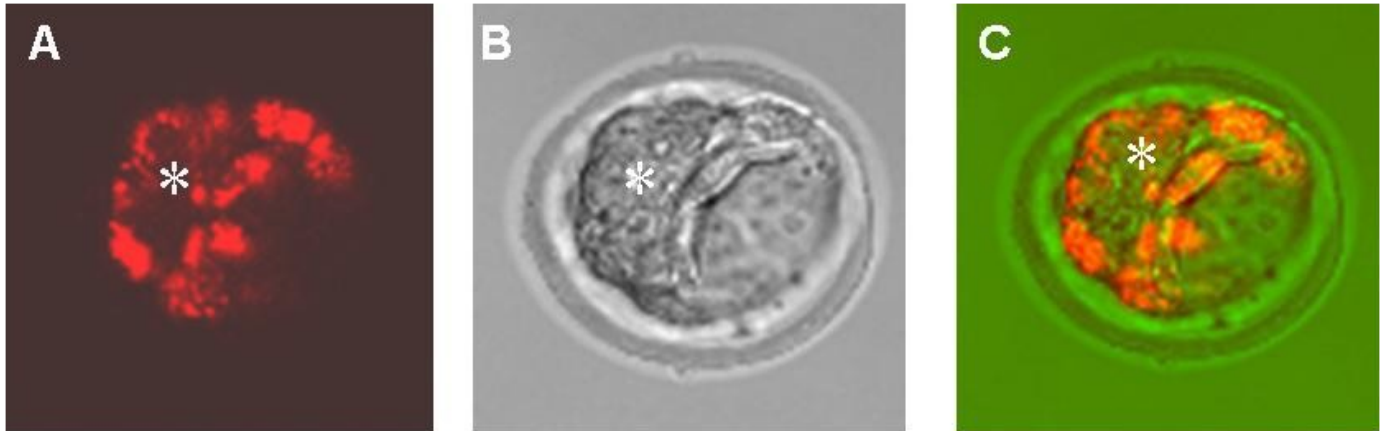


Figure 1. In vitro uptake of Cy3-crotamine in developing blastocyst. A–C Strong fluorescent signal observed within the inner cell mass of blastocyst (asterisk). **(A)** = fluorescent confocal microscopy (Fcm); **(B)** = digital interference contrast (Dic); **(C)** = overlay of Dic+Fcm; magnification 250 \times .

Fig. 2

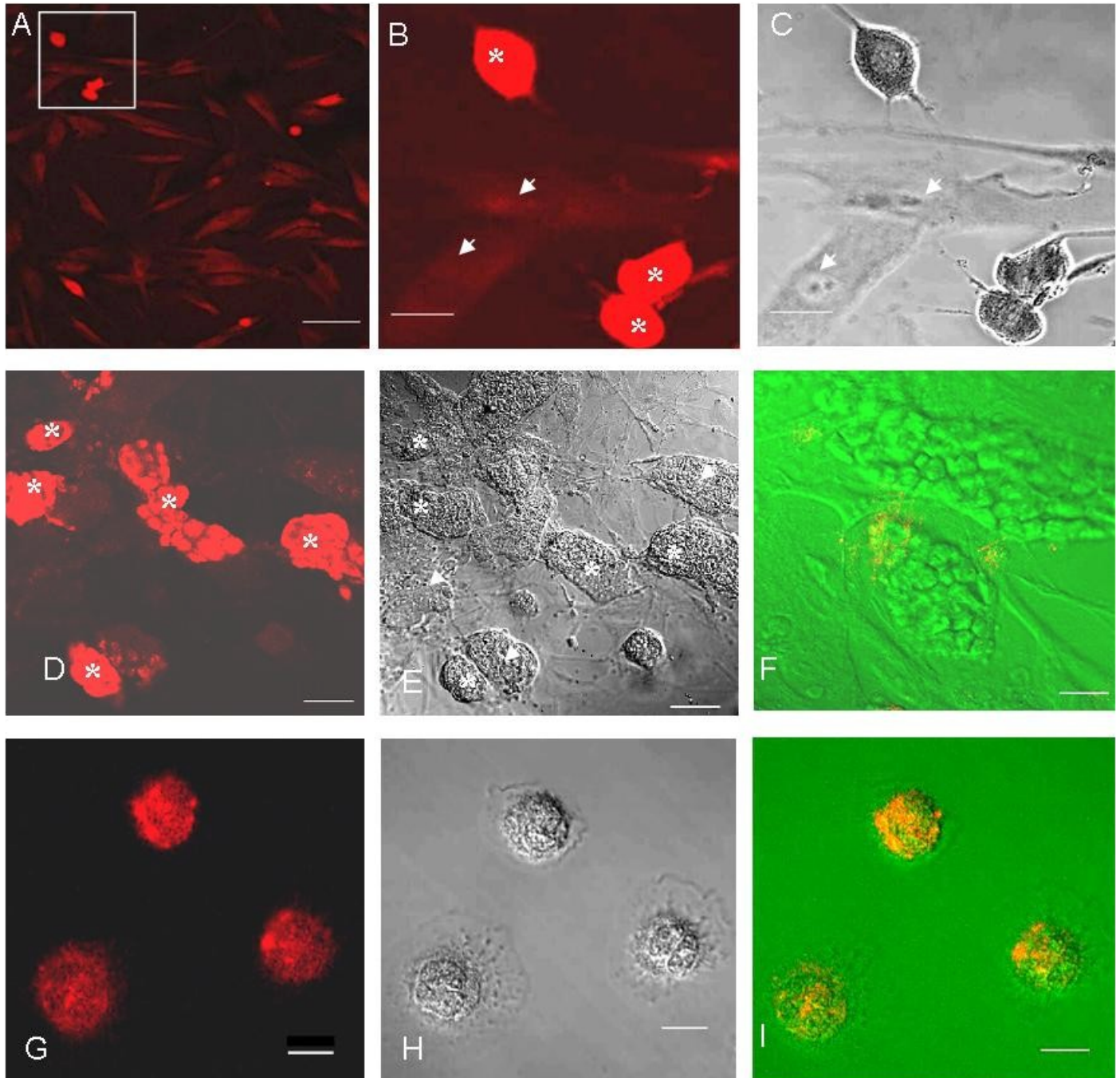


Figure 2. In vitro and in vivo uptake of Cy3-crotamine in different cell types. *A*) In vitro crotamine uptake after 1 h treatment in human fibroblasts; inset shows rounded up, supposedly dividing cells (Fcm; bar = 100 μ m). *B*, *C*) Higher magnification of inset in (*A*): dividing cells (asterisk) are strongly labeled with crotamine, whereas a weak signal is observed in quiescent cells (arrowhead; *B* = Fcm; *C* = Dic; bars = 25 μ m). *D*, *E*) Pluripotent ES cells with strong (asterisk) and weak crotamine-labeling (arrowhead) observed within the islands (*D* = Fcm; *E* = Dic; bars = 100 μ m). *F*) Control cultured ES cells treated with Cy3 dye for 3 h, showing a weak background fluorescence (Dic+Fcm; bar = 100 μ m). *G–I*) In vivo crotamine uptake observed 3 h after injection into mice: peritoneal liquid cells show strong fluorescence in the perinuclear space and in the nuclei. (*G* = Fcm, *H* = Dic, *I* = Dic+Fcm; bars = 100 μ m).

Fig. 3

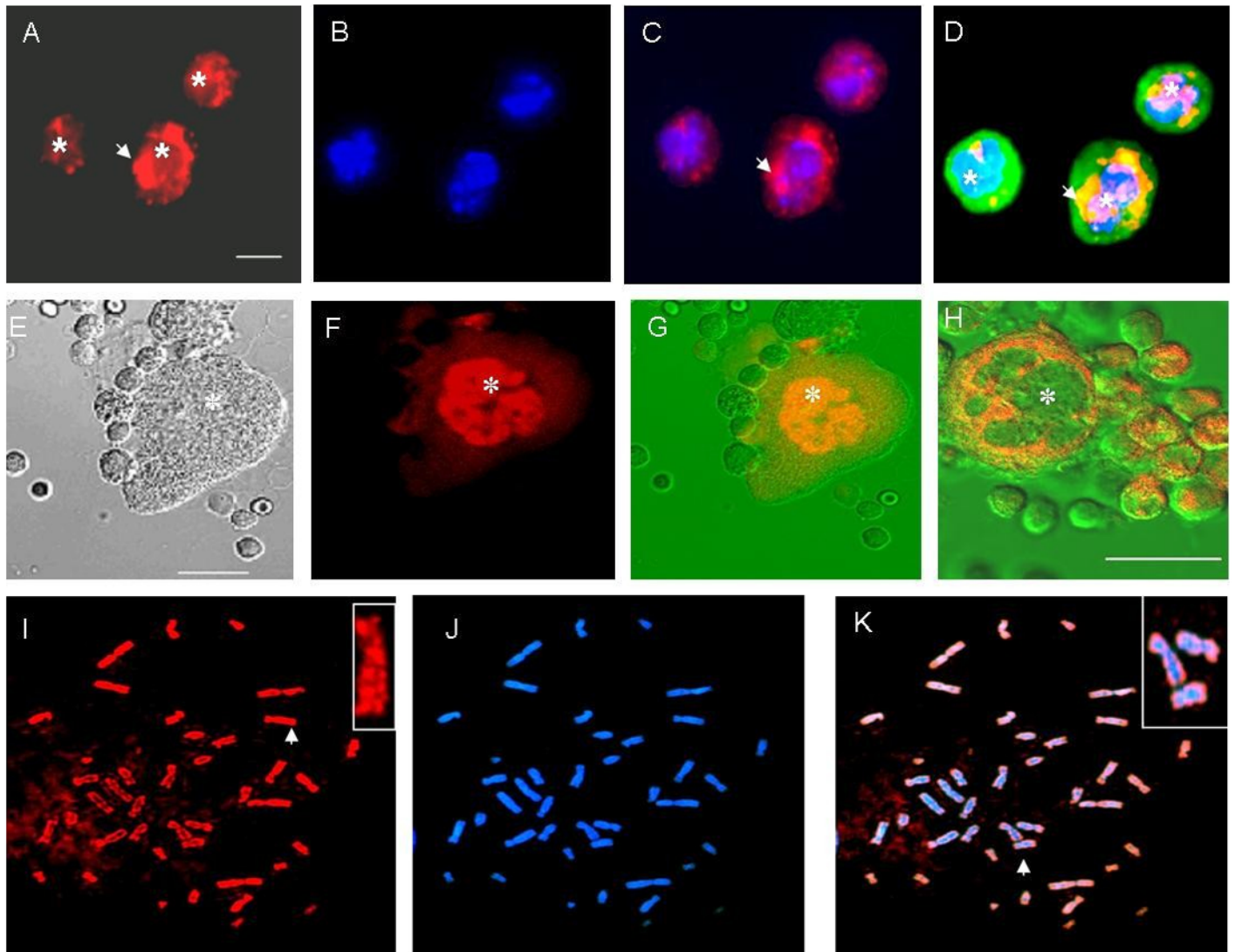


Figure 3. In vitro and in vivo nuclear localization of Cy3-crotamine and its association with mitotic chromosomes. *A–D*) Internalization of Cy3-crotamine, 3 h after injection into mice, observed in nuclei (asterisk) and perinuclear space (arrow) of peritoneal liquid cells. *A*) Cy3-crotamine. *B*) Nuclei stained by DAPI (blue). *C*) Superimposed images (*A*) and (*B*): partial overlapping (pink) of Cy3-crotamine localization (red) and DAPI staining in nuclei (arrow). *D*) Superimposed images (*A*) and (*B*), demonstrating overlapping (pink) of Cy3-crotamine localization and DAPI staining within the nuclei, and overlapping (yellow) of cytoskeleton immunostained with anti-tubulin antibody (green) and Cy3-crotamine in perinuclear space (*A–D*= Epifluorescence, EF; bar = 50 μ m). *E–G*) Cy3-crotamine strong labeling in nucleus (asterisk) and weak fluorescence in cytoplasm of mouse megakaryocyte (*E* = Dic, *F* = Fcm, *G* = Dic + Fcm; bars = 25 μ m). *H*) Cells pretreated with non-labeled crotamine followed by Cy3-crotamine treatment. Strong fluorescence restricted to the cytoplasm indicates saturation of binding sites by non-labeled crotamine in the nucleus (asterisk), as clearly observed in the megakaryocyte (Dic + Fcm; Bar = 10 μ m). *I–K*) Metaphase of lymphoblastic cell. (EF; Magnification, 800 \times). *I*) Cy3-crotamine labeled chromosomes. A banding pattern is produced as shown by the chromosome in the inset. *J*) DAPI-stained chromosomes. *K*) Superposition of images (*I*) and (*J*): Crotamine labeling (red) is observed on DAPI-stained chromosomes. In the inset, the association of crotamine with DAPI-stained chromosomes is depicted (arrow).

Fig. 4

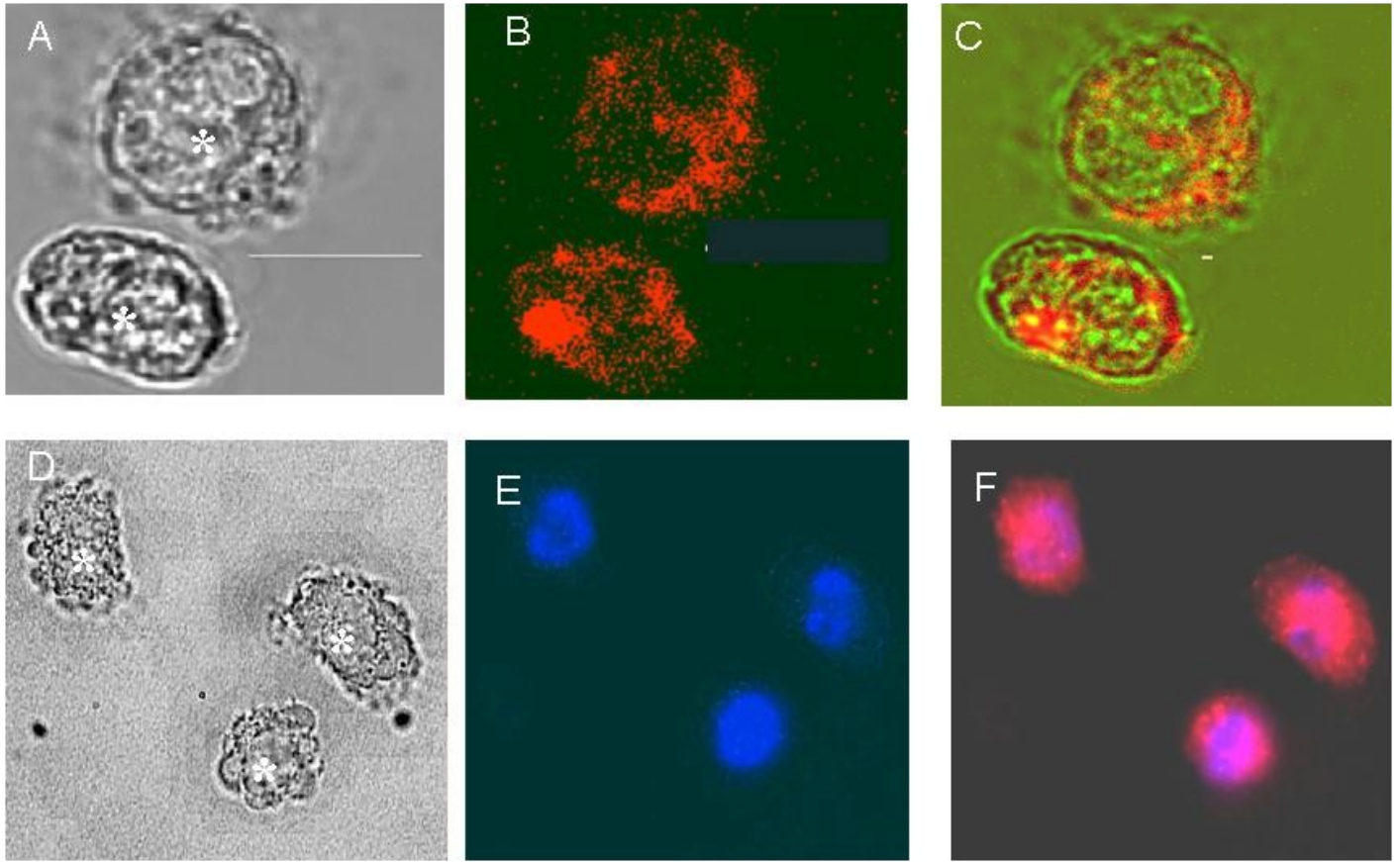


Figure 4. Uptake of Cy3-crotamine demonstrated in unfixed cells. *A–F*) Unfixed peritoneal liquid cells. *A–C*) Fluorescence observed in the nuclei (asterisk) and perinuclear space (*A* = Dic, *B* = Fcm, *C* = Dic+Fcm; bars = 5 µm). *D–F*) Cy3-crotamine localization in the DAPI-stained nuclei. *D*) Nuclei (asterisk) observed in phase contrast. *E*) DAPI-stained nuclei. *F*) Cy3-crotamine fluorescence (red) and DAPI-staining (blue) partially overlap (pink; EF, magnification 800×).

Fig. 5

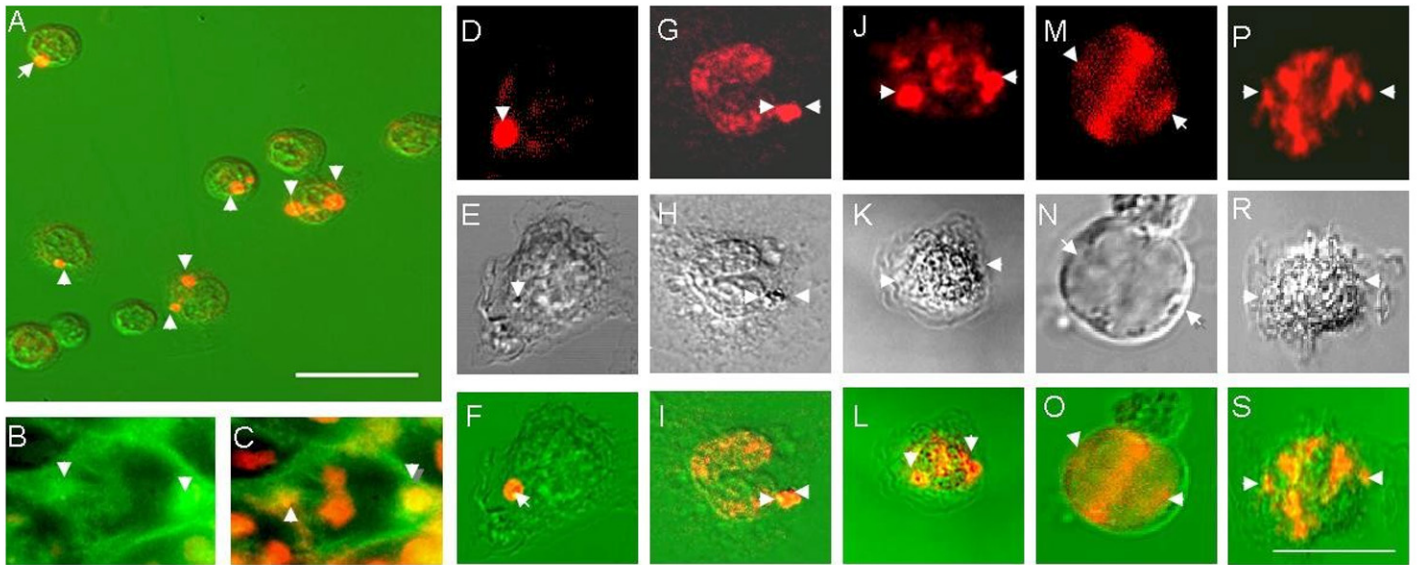


Figure 5. Cy3-crotamine as a marker of centrioles in living cells. *A*) Peritoneal liquid cells showing Cy3-crotamine fluorescence on centrosomes (arrowheads). (Dic + Fcm; bar = 100 μ m). *B*) Microtubules and esters (arrowheads) immunolabeled by anti α -tubulin (green) in pluripotent ES cell. *C*) Superimposed images of centrioles labeled by Cy3-crotamine (red) and esters immunolabeled by anti α -tubulin (green): the yellow labeling of the centrioles results from the superposition of red and green labels). Chromosomes are strongly labeled (red) by crotamine. (*B*, *C* = Fcm; bars = 10 μ m). *D–S*) Centriole labeling (arrowheads) by Cy3-crotamine in peritoneal liquid cells. *D–F*) In G1 phase, pericentriolar material associated with a pair of centrioles is strongly labeled by crotamine. *G–I*) In S/G2 phase the duplicated centrioles start to separate. Fluorescence is also observed in the cell nucleus. *J–L*) In prophase, the two centrioles are moving to opposite poles. Crotamine binding to chromosomes becomes evident. *M–O*) In metaphase and (*P–S*) anaphase strong fluorescence is observed on centrioles and on chromosomes. (*D*, *G*, *J*, *M*, *P* = Fcm; *E*, *H*, *K*, *N*, *R* = Dic; *F*, *I*, *L*, *O*, *S* = Dic + Fcm; bars = 10 μ m).

Fig. 6

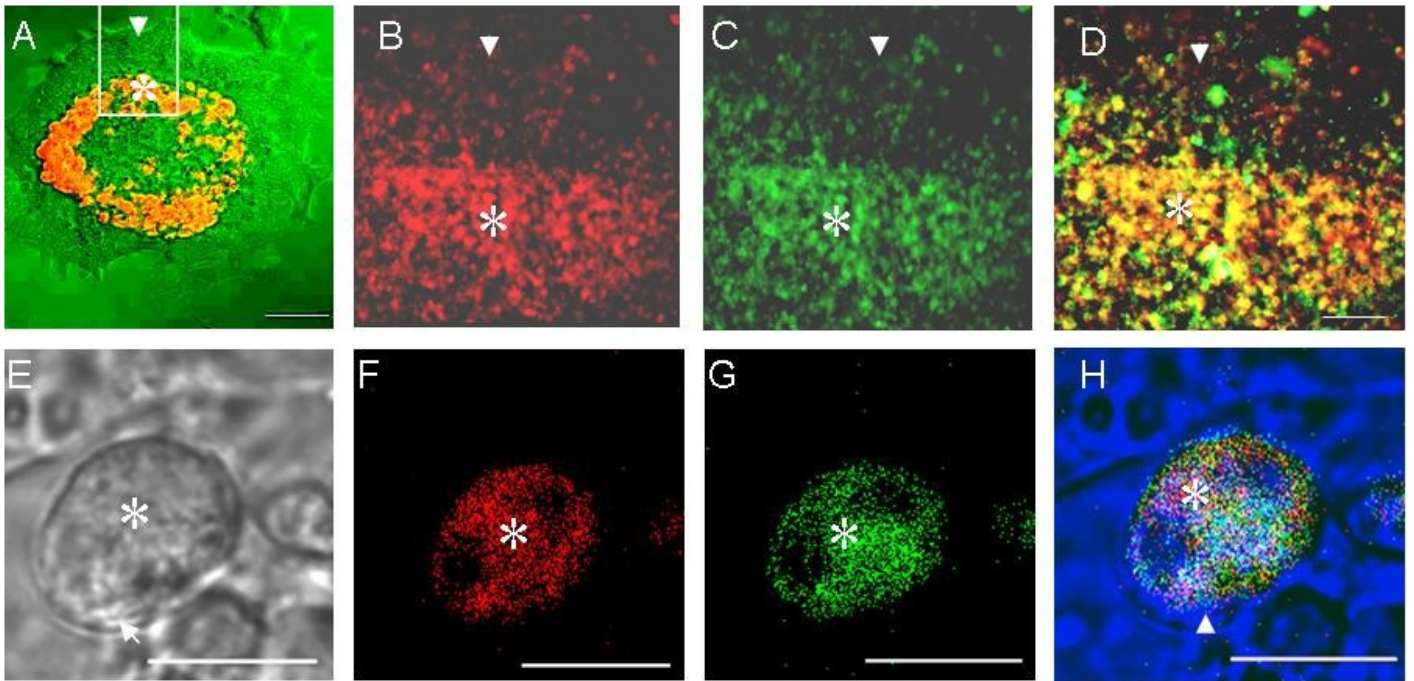


Figure 6. Uptake of Cy3-crotamine into actively proliferating cells. *A–D*) Differentiating Ebs. *A*) Area of undifferentiated ES cells (asterisk) shows strong fluorescence. Area of weakly fluorescent differentiated ES cells (arrowhead). (Dic + Fcm, bar = 100 μm .) *B*) Higher magnification of inset from (*A*): Crotamine uptake is intensive in undifferentiated (asterisk) and weak in differentiated (arrowhead) ES cells. *C*) Same as in (*B*): High 5-BrdU incorporation, demonstrated by FITC-conjugated anti-BrdU antibody, indicates actively proliferating ES cells (asterisk); and an area of predominantly non-dividing cells (arrowhead). *D*) Superimposed images of (*B*) and (*C*): overlapping (yellow) of intensive crotamine (red) internalization and 5-BrdU (green) incorporation by actively proliferating cells (*B–D* = Fcm; bars = 25 μm .) *E–H*) Undifferentiated ES cell. *E*) ES cell morphology (asterisk, nucleus; arrow, cytoplasm). *F*) Cy3-crotamine (red) within the nucleus. *G*) 5-BrdU (green) within the nucleus. *H*) Superimposed images (*F*) and (*G*): partial overlapping (yellow) of Cy3-crotamine internalization and 5-BrdU incorporation in the nucleus (*E* = Dic; *F*, *G* = Fcm; *H* = Dic + Fcm; bars = 10 μm .)